

# A state-space simplified SCR catalyst model for real time applications

Claes Ericson, Björn Westerberg  
Scania CV AB

Ingemar Odenbrand  
Chemical Engineering, LTH, Lund University

Copyright © 2008 SAE International

## ABSTRACT

The use of Selective Catalytic Reduction (SCR) is becoming increasingly more popular as a way of reducing NO<sub>x</sub> emissions from heavy duty vehicles while maintaining competitive operating costs. In order to make efficient use of these systems, it's important to have a complete system approach when it comes to calibration of the engine and aftertreatment system. This paper presents a simplified model of a heavy duty SCR catalyst, primarily intended for use in combination with an engine-out emissions model to perform model based offline optimization of the complete system.

The traditional way of modelling catalysts using a dense discretization of the catalyst channels and non-linear differential equation solvers to solve the heat and mass balance equations, requires too much computational power in this application. The presented model is also useful in other applications such as model based control. The basic model structure is a series of continuously stirred tank reactors using discretized catalyst walls to describe the mass transport in the solid phase. The simplified model uses a state-space concept. At low temperatures the model uses an implicit method of calculating the coverage differential. At higher temperatures, the model is simplified to a first order system using an operating condition dependent characteristic time constant. These simple, yet robust methods allows for long step lengths in the process of solving the differential equations. This makes the model a useful improvement over current models.

## INTRODUCTION

With the introduction of Euro 4 emission standards for heavy trucks in Europe, the use of Selective Catalytic Reduction (SCR) using Urea/AdBlue as reduction agent is now an industry standard. Control and optimization of such systems is not trivial though. In order to reach future emission standards such as Euro 6 and EPA 10, high conversion rates over the catalyst must be achieved in all operating conditions. A novel approach to solve these problems is to use model based control and optimization. The models should preferably be of such simplicity that they can be executed in real time in the engine control system or millions of times in a short time span in the process of offline optimization. Previous efforts using model based control of the SCR catalyst have shown promising results with an average conversion of 84% over the FTP test cycle [1].

To achieve even better performance, models of both the engine and catalyst can be combined to get a complete system approach. In a previous paper, a model of a heavy truck diesel engine equipped with common rail fuel injection, cooled EGR and a variable geometry turbocharger (VGT) was presented [2]. The corresponding SCR catalyst model is introduced in this paper. The modelled catalyst is a vanadina-based SCR catalyst of typical heavy truck dimensions. Similar catalyst models have been around for more than a decade [3, 4]. The problem with this latter type of models is the short step length required (in the process of solving the differential equations) to maintain stability at high temperatures and/or high dosing strategies. The simplified model uses a less dense discretization and alternate methods of updating the coverage states, which allows for substantially longer step lengths.

## MODELS

In this section the SCR catalyst model in its original and simplified form is introduced.

### THE ORIGINAL MODEL

The catalyst is modeled as a series of continually stirred tank reactors. The walls are discretized into a number of layers to describe the mass transport through the walls, as illustrated in Figure 1. The model uses 3 wall layers and 6 segments (tanks) in the axial direction.

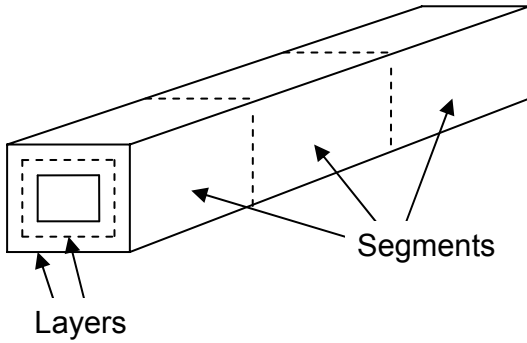
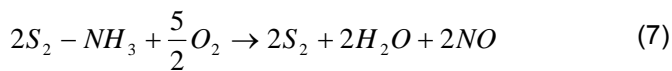
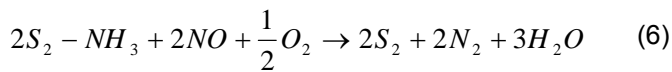
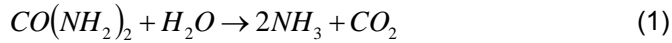


**Figure 1** Illustration of the catalyst discretization principle

Uniform radial flow and concentration distribution over the catalyst cross section is assumed; therefore it's sufficient to model one channel only. Axial diffusion and the radial temperature gradients are both neglected.

The reaction mechanism consists of seven reactions:



$S_i$  denotes an active site on the catalyst surface. Typically, the activation energy for desorption of ammonia is reduced with increasing coverage. This can be modeled as a Temkin-type linearly decreasing activation energy [5]. Another approach, as applied in this model, is to use two types of sites with different activation energies. The surface reactions are of the Eley-Rideal type. Reaction 1 describes the decomposition of urea to ammonia. The adsorption / desorption (accumulation) of ammonia is given by reactions 2, 3, 4 and 5. The desired reaction, NO-reduction on the active sites is described by reaction 6.

Finally, at higher temperatures, unwanted ammonia oxidation also occurs on the sites (reaction 7).

### Reaction rates

The corresponding reaction rates are given by:

$$r_1 = k_1 c_{Urea} \quad (8)$$

$$r_2 = k_2 c_{NH_3} \theta_{1,v} \quad (9)$$

$$r_3 = k_3 \theta_{1,NH_3} \quad (10)$$

$$r_4 = k_4 c_{NH_3} \theta_{2,v} \quad (11)$$

$$r_5 = k_5 \theta_{2,NH_3} \quad (12)$$

$$r_6 = k_6 c_{NO} \theta_{2,NH_3} \quad (13)$$

$$r_7 = k_7 \theta_{2,NH_3} \quad (14)$$

where

$$\theta_{x,v} = 1 - \theta_{x,NH_3} \quad (15)$$

The rate coefficients  $k_j$  are calculated using an Arrhenius type expression:

$$k_j = k_{0,j} e^{\frac{E_{A,j}}{RT_s}} \quad (16)$$

where  $j$  is the reaction number,  $k_{0,j}$  is the pre exponential factor,  $E_{A,j}$  is the activation energy,  $R$  is the molar gas constant and  $T_s$  is the surface temperature.

### Balance equations

The axial flow and the radial diffusion are both modeled using static balance equations for the gas phase and time dependent balances for the solid catalyst. This results in a set of partial differential equations. The gas phase mass balances are given by:

$$F_{tot} (y_{i,k-1} - y_{i,k}) - \Gamma_{i,k,0} (c_{i,k,0} - c_{i,k,1}) = 0 \quad (17)$$

$$\Gamma_{i,k,n-1} (c_{i,k,n-1} - c_{i,k,n}) - \Gamma_{i,k,n} (c_{i,k,n} - c_{i,k,n+1}) + \sum_j v_{i,j} r_{j,k,n} w_{k,n} = 0 \quad for \quad n \geq 1 \quad (18)$$

where  $F_{tot}$  is the total molar flow,  $c_{i,k,n}$  is the concentration of component  $i$  in channel segment  $k$  and wall layer  $n$  (where  $n=0$  indicates gas bulk and  $n>0$  indicates wall) and  $w_{k,n}$  is the mass of catalyst material in channel segment  $k$  and wall layer  $n$ . The mass transfer coefficients  $\Gamma_{i,k,n}$  are given by:

$$\Gamma_{i,k,0} = \frac{A_k}{\frac{1}{k_{c,i,k}} + \frac{0.5\Delta x_1}{D_{eff,i,k}}} \quad (19)$$

$$\Gamma_{i,k,n} = \frac{D_{eff,i,k} A_k}{0.5\Delta x_n + 0.5\Delta x_{n+1}} \quad (20)$$

for  $n=1 \dots N-1$

$$\Gamma_{i,k,N} = 0 \quad (21)$$

where  $A_k$  is the mass and heat transfer area in channel segment  $k$ . For simplicity reasons,  $A_k$  is assumed to be constant for all wall layers.  $D_{eff,i,k}$  is the effective pore diffusion coefficient of component  $i$  in channel segment  $k$ ,  $k_{c,i,k}$  is the film transfer coefficient of component  $i$  in channel segment  $k$  and  $\Delta x_n$  is the thickness of wall layer  $n$ .

The surface mass balances are given by:

$$N_c \frac{d\theta_{x,NH_3,k,n}}{dt} = \sum_j v_{NH_3,j} r_{j,k,n} \quad (22)$$

where  $v_{NH_3,j}$  is the stoichiometric coefficient for ammonia in reaction  $j$ ,  $r_{j,k,n}$  is the rate of reaction  $j$  in channel segment  $k$  and wall layer  $n$ ,  $N_c$  is the number of active sites per kg catalyst,  $\theta_{x,NH_3,k,n}$  is the ammonia coverage on site  $x$  in channel segment  $k$  and wall layer  $n$  and  $t$  is the time. The gas energy balance is given by:

$$F_{tot} c_{p,g} (T_{g,k-1} - T_{g,k}) - h_k A_k (T_{g,k} - T_{s,k}) = 0 \quad (23)$$

where  $c_{p,g}$  is the heat capacity for the gas,  $h_k$  is the heat transfer coefficient in channel segment  $k$ ,  $T_{g,k}$  and  $T_{s,k}$  are the temperatures in channel segment  $k$  in the gas bulk and of the catalyst respectively. The solid energy balance is given by:

$$m_{s,k} c_{p,s} \frac{dT_{s,k}}{dt} = h_k A_k (T_{g,k} - T_{s,k}) - A_s (q_{k+1} - q_k) + \sum_n \sum_j r_{j,k,n} w_{k,n} (-\Delta H_j) \quad (24)$$

where  $m_{s,k}$  is the total mass of solid material in channel segment  $k$ ,  $c_{p,s}$  is the heat capacity of the solid material,  $A_s$  is the cross sectional area of the catalyst wall,  $w_{k,n}$  is the mass of active catalyst material in channel segment  $k$  and wall layer  $n$  and  $-\Delta H_j$  is the heat of reaction  $j$ . The solid heat flux is calculated as:

$$q_k = -2\lambda_s \frac{T_{s,k} - T_{s,k-1}}{\Delta z_k + \Delta z_{k-1}} \quad \text{for } k = 2 \dots K-1, K \quad (25)$$

$$q_k = 0 \quad \text{for } k = 1, K+1 \quad (26)$$

where  $\lambda_s$  is the heat conductivity for the solid material,  $\Delta z_k$  is the length of channel segment  $k$  and  $K$  is the total number of channel segments. The mass and heat transfer is described with the film model and the mass and heat transfer coefficients are given by:

$$k_{c,i,k} = \frac{Sh D_{i,k}}{d} \quad (27)$$

$$h_k = \frac{Nu \lambda_g}{d} \quad (28)$$

where  $D_{i,k}$  is the diffusion coefficient for component  $i$  in channel segment  $k$ ,  $\lambda_{g,k}$  is the gas heat conductivity in channel segment  $k$  and  $d$  is the channel width.  $Sh$  and  $Nu$  are the Sherwood and the Nusselt number respectively. The asymptotic values for  $Sh$  and  $Nu$  are used (entrance effects are neglected). Asymptotic values are given by Tronconi et al [7].

### Gas diffusivity

The gas diffusivity for each component  $i$  is calculated using a simplified form of the Fuller-Schettlet-Giddins equation [6]:

$$D_i = D_{ref,i} \left[ \frac{T_s}{T_{ref}} \right]^{1.75} \quad (29)$$

where  $T_{ref}$  is a reference temperature. The effective diffusivity for pore diffusion is given as:

$$D_{eff,i} = \frac{f_D}{\frac{1}{D_i} + \frac{1}{D_{K,i}}} \quad (30)$$

$f_D$  is a factor that takes into consideration the porosity and the tortuosity of the porous material.  $D_{K,i}$  is the Knudsen diffusivity which is calculated as:

$$D_{K,i} = \frac{d_p}{3} \sqrt{\frac{8RT_s}{\pi M_i}} \quad (31)$$

where  $d_p$  is the mean pore diameter.

### THE SIMPLIFIED MODEL

The first simplification is to use only one type of active sites. In other words, reactions 2 and 3 are omitted. The number of wall layers is reduced to 2 to reduce the total number of states to 18 compared to 42 for the original model. The accuracy of the model will still be adequate, as discussed in the results section. One important advantage of using fewer wall layers is stability; longer step lengths are possible, thus improving computational efficiency. The original model in a fixed step length implementation uses short step lengths, typically 50ms or less in order to avoid stability problems at high temperatures. It would be desirable to use longer steps though since the dynamics of the catalyst as a whole is substantially slower. The limiting factor for taking long steps is the fast dynamics of the thin surface wall layer. The dynamics of the second wall layer and the energy balance is much slower.

The models are implemented using the Euler method:

$$\theta_{k,n}(t + \Delta t) = \theta_{k,n}(t) + \Delta t \frac{d\theta_{k,n}}{dt} \quad (32)$$

From equation 31 and on, the  $NH_3$  and  $x$  indexes on the coverage variable are dropped for a more compact representation. Implicit methods can be applied to get more accurate steps and thus enable longer step lengths. For the first layer the coverage differential is given by:

$$\frac{d\theta_{k,1}}{dt} = \frac{1}{N_c} (r_{4,k,1}(t) - r_{5,k,1}(t) - 2r_{6,k,1}(t) - 2r_{7,k,1}(t)) \quad (33)$$

The implicit method uses the second layer concentrations and surface temperature from the previous time step, and the updated coverage according to equation 31 for calculating the reaction rates. The first layer concentrations are given by the mass balances (equations 19-21), also using the updated coverage. The result is a third degree polynomial:

$$\beta_1 \left( \frac{d\theta_{k,1}}{dt} \right)^3 + \beta_2 \left( \frac{d\theta_{k,1}}{dt} \right)^2 + \beta_3 \left( \frac{d\theta_{k,1}}{dt} \right) + \beta_4 = 0 \quad (34)$$

where

$$\beta_m = \beta_m(\Delta t, \theta_{k,1}(t), c_{i,k-1,0}(t + \Delta t), c_{i,k-1,2}(t), F(t + \Delta t), T_s(t)) \quad (35)$$

The polynomial is easily solved using analytical methods. Choosing which root to use is simple; only one is physically possible. The implicit method improves stability, as will be discussed in the results section. The second layer coverage is updated using the kinetic expression (equation 22).

Another method to improve high temperature stability is to simplify the system to a first order system approaching a steady state solution  $\theta_{ss}$  in each time step [6]. The coverage is given by:

$$\frac{d\theta_{k,1}}{dt} = \frac{\theta_{ss,k,1} - \theta_{k,1}}{\tau} \quad (36)$$

where  $\theta_{ss,k,1}$  is the steady state solution corresponding to the current inputs and  $\tau$  is a characteristic time constant. The steady state solution can be estimated by solving a simplified version of the gas phase mass balances (equations 17-18). At high temperatures the system is mass transport limited which allows for a number of simplifications. The simplifications consist of assuming that all urea is decomposed and all ammonia reacts with NO before reaching the second layer:

$$c_{Urea,k,2} = 0 \quad (37)$$

$$c_{NH_3,k,2} = 0 \quad (38)$$

A simple approximation for the second layer NO concentration is also applied:

$$c_{NO,k,2} = \max(0, c_{NO,k-1,0} - c_{NH_3,k-1,0} - 2c_{Urea,k-1,0}) \quad (39)$$

By combining the simplified gas phase mass balances with equilibrium in the surface mass balances, i.e.:

$$r_{4,k,1} - r_{5,k,1} - 2r_{6,k,1} - 2r_{7,k,1} = 0 \quad (40)$$

, the result is a third degree polynomial:

$$\alpha_1 (\theta_{ss,k,1})^3 + \alpha_2 (\theta_{ss,k,1})^2 + \alpha_3 (\theta_{ss,k,1}) + \alpha_4 = 0 \quad (41)$$

where

$$\alpha_m = \alpha_m(c_{i,k-1,0}(t + \Delta t), F(t + \Delta t), T_s(t)) \quad (42)$$

This polynomial is also solved using analytical methods, and only one root is physically possible. Note that the simplifications are only valid at high temperatures. Empirically, for the catalyst studied, it has been shown that above approximately 700K, the simplifications results in good accuracy. Further, the second layer coverage is set to zero, consistent with equations 37 and 38.

Using an empirically determined black-box model, the time constant is estimated:

$$\tau_{k,1} = \tau_{k,1}(T_{s,k}, \theta_{ss,k,1}, c_{NO,k,1}, c_{NH_3,k,1}, c_{Urea,k,1}) \quad (43)$$

The simplified model combines the two methods; at lower temperatures the implicit method is used, and at higher temperatures the first order simplification is used. The temperature states are in both cases updated using the kinetic expression (equation 24). The algorithm can be illustrated with the following flowchart:

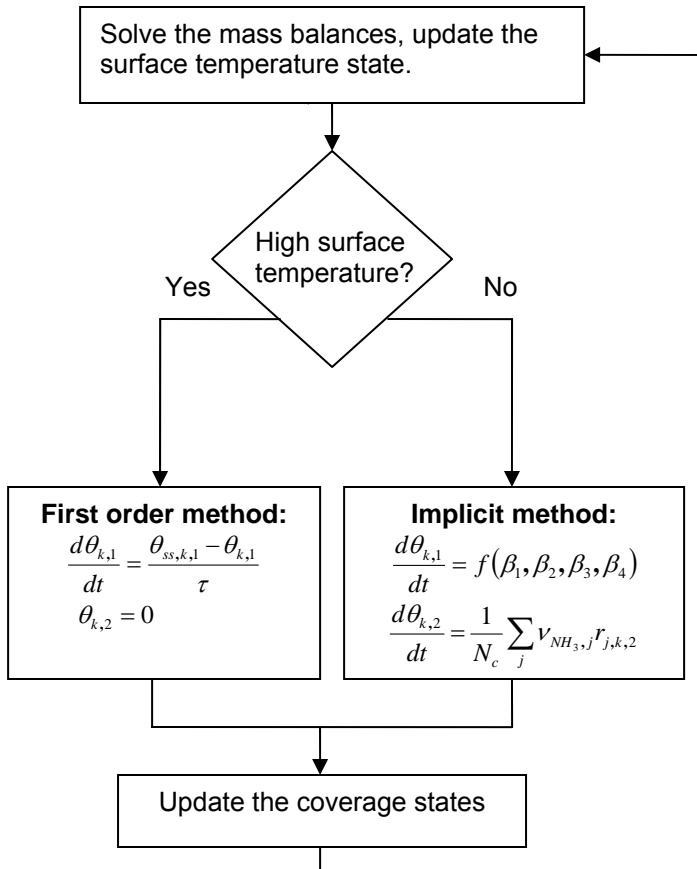


Figure 2 Flowchart of the simplified model

Note that the model in some cases will operate simultaneously in different modes depending on the segment temperature.

## RESULTS

In this section the original and simplified models will be validated and compared using measurement data from an experimental engine.

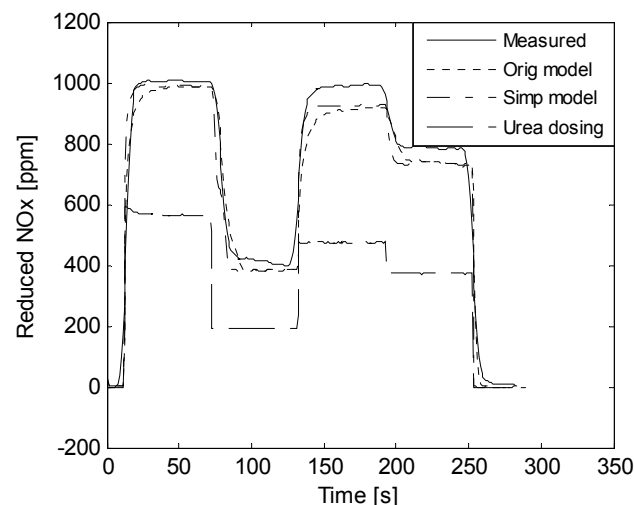


Figure 3 Step response experiment, 670K exhaust temperature, model comparison

The original and simplified models are compared in Figure 3 which shows one of the step sequence experiments used to fit the model parameters. To determine the accuracy of the model structure as such and avoid step length influences, variable step lengths are used in all simulations. The models are implemented in Matlab (uncompiled code). Both models are fitted with adequate results, although the original model gets a slightly lower sum of squares in the optimization process. The experiment is performed at constant exhaust temperature (670K), flow (8 mole/s) and NO<sub>x</sub> concentration (1000ppm) with steps in the urea dosing. Validating the models using a measured transient test cycle (ETC) however shows the opposite results; the simplified model is actually a better fit to measured values. This could be related to that the more complex original model is sub-optimized to the step experiments used for parameter tuning. Another possibility is measurements error of the ETC experiment. Figure 4 and Figure 5 shows comparisons of the two models. The engine is calibrated for low NO<sub>x</sub> levels and a low exhaust temperature of less than 650K in all points.

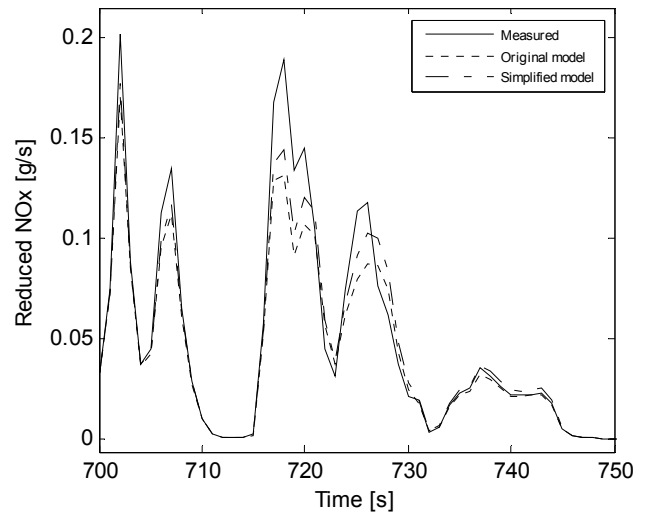


Figure 4 Sequence 1 of the ETC, model comparison

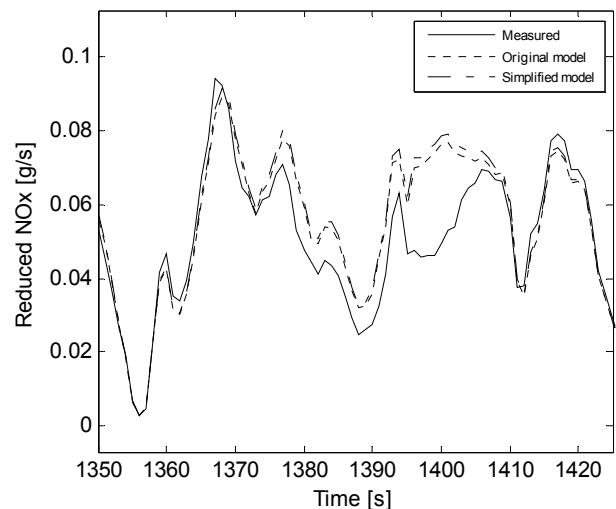
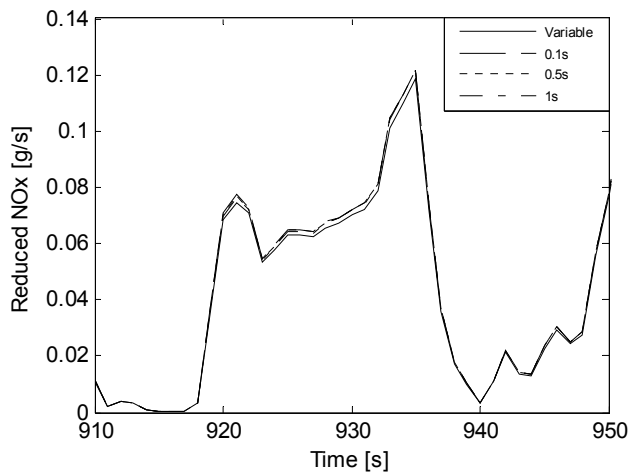


Figure 5 Sequence 2 of the ETC, model comparison

The influence of step lengths was studied by running a number of simulations. The results are shown in Figure 6 and Table 1.



**Figure 6** Sequence of the ETC, step length comparison

The difference between different step lengths up to 1s and variable step length is negligible.

**Table 1** Step length comparison, ETC cycle

Step	Deviation	Execution time
0.1s Implicit (ref.)	0%	212.5
0.5s Implicit	0.46%	20.8
1s Implicit	1.05%	10.3

The second column is the mean relative error in reduced  $\text{NO}_x$  compared to the 0.1s implicit step reference. The mean relative error between the reference step length and a variable step implementation is 3.3%. Variable step length is not a viable option in engine control system applications though and also makes the integration with the engine model more complicated. The simulations were performed on a 1.6GHz PC. Note that the model is substantially faster than real time. Also, the computational performance can be improved considerably using longer steps with small increases in the mean relative error. To ensure stability up to 720K where the switch between the implicit and first order modes are made in the simplified model, a 0.5s step length is a good choice.

In order to validate the high temperature performance of the model, a step response experiment similar to the one depicted in figure 3 although at a higher exhaust temperature (760K) was performed. At those temperatures, the simplified model uses the first order method. Figure 7 shows the results of the simulations.

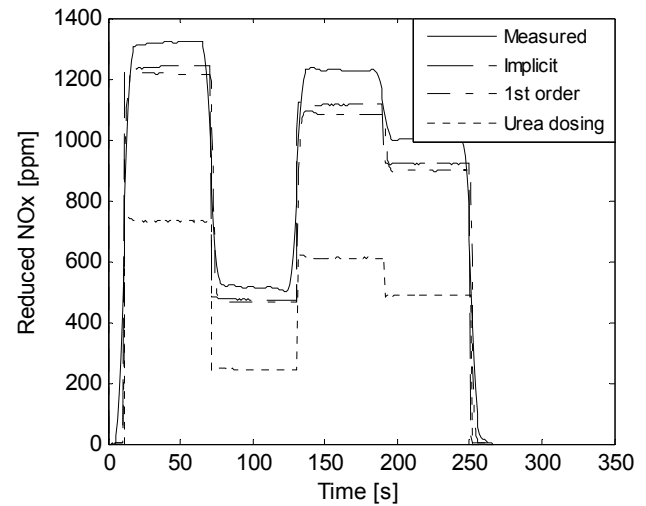


**Figure 7** Step response experiment, 760K exhaust temperature, validation of the first order method

The first order method is executed using a 0.5s step length and is compared with the implicit method and measured data. The step can be increased to 1s with little increase in mean relative error. The agreement is good, although the implicit method produces slightly better results. Note that if the implicit method is used, the step length must be reduced to approximately 0.1s to avoid oscillations and instabilities. If the exhaust temperature is increased further to 800K or more, the step must be further reduced to retain stability. Thus substantial improvements in computational efficiency can be achieved by switching to the first order method at high temperatures.

## CONCLUSIONS

A simplified SCR catalyst model has been presented. The model uses a discretization of the monolith channels with six segments in the axial direction and two (wall) layers in the radial direction. An implicit method to calculate the ammonia coverage differential is applied at temperatures up to 720K and a first order simplification is used at higher temperatures. This allows for a 0.5s step length while maintaining stability in all operating cases.

The execution time for a complete ETC is 20.8 seconds on a 1.6GHz computer using uncompiled Matlab code, thus the model operates substantially faster than real time. Real time performance should be possible in computers of similar computational power as the current engine control systems. The fast performance also makes the model an excellent candidate for offline optimization purposes.

The agreement with measurements is of the same order as previous, more complex models. This makes the simplified model a useful improvement.

## ACKNOWLEDGMENTS

This work was partly financed by the Emission Research Programme (EMFO). EMFO is supported by the Swedish National Road Administration, the Swedish Agency for Innovation systems and the Swedish Energy Agency. The authors would also like to acknowledge all the people at Scania Engine Development who were helpful with the measurements.

## REFERENCES

1. Chi, J. Dacosta, H. "Modeling and Control of a Urea-SCR Aftertreatment System", SAE Technical papers 2005-01-0966, 2005.
2. Ericson, C. Andersson, M. Egnell, R. Westerberg, B. "Modelling diesel engine combustion and NO<sub>x</sub> formation for model based control and simulation of engine and exhaust aftertreatment system", SAE Technical papers 2006-01-0687, 2006.
3. Andersson, L. Gabrielsson, P and Odenbrand, I "Reducing NO<sub>x</sub> in Diesel Exhausts by SCR Technique: Experiments and Simulations", A.I.Ch.E. J., 40, 1994.
4. Andersson, L. "Mathematical Modelling in Catalytic Automotive Pollution Control", Doctoral Thesis, Department of Chemical Reaction Engineering, Chalmers University of Technology, 1995.
5. Ciardelli, C. Nova, I. Tronconi, E et. al. "SCR-DeNOx for diesel engine exhaust aftertreatment: unsteady-state kinetic study and monolithic reactor modelling", Chemical Engineering Science 59, 2004.
6. Murzin, D. Salmi, T "Catalytic Kinetics", pp. 408, 285-288, Elsevier, Amsterdam, 2005.
7. Tronconi, E. and Forzatti, P. "Adequacy of Lumped Parameter Models for SCR Reactors with Monolith Structure", AIChE Journal 38, 1992.

## CONTACT

claes.ericson@scania.com

## DEFINITIONS, ACRONYMS, ABBREVIATIONS

VGT Variable geometry turbocharger  
 SCR Selective catalytic reduction  
 EGR Exhaust gas recirculation

$r_i$	[mol/s kg cat]	Reaction rate, reaction i
$k_i$	[m <sup>3</sup> /s kg cat] / [mol/s kg cat]	Rate coefficient, reaction i
$k_{0,i}$	[m <sup>3</sup> /s kg cat] / [mol/s kg cat]	Preexponential factor, reaction i
$E_{A,i}$	[J/mol]	Activation energy, reaction i
$R$	[J/mol K]	Molar gas constant
$\theta_{x,i}$	[1]	Coverage of specie i, site x
$c_i$	[mol/m <sup>3</sup> ]	Concentration, specie i
$y_i$	[1]	Molar fraction, specie i
$F_{tot}$	[mol/s]	Total molar flow
$\Gamma_{l,k,n}$	[m <sup>3</sup> /s]	Mass transfer coefficient, specie i in layer n, segment k
$D_i$	[m <sup>2</sup> /s]	Diffusivity, specie i
$D_{K,i}$	[m <sup>2</sup> /s]	Knudsen diffusivity, specie i
$D_{eff,i}$	[m <sup>2</sup> /s]	Effective diffusivity, specie i
$f_D$	[1]	Porosity-tortuosity factor
$\nu_{i,j}$	[1]	Stoichiometric factor, specie i in reaction j
$w_{k,n}$	[kg]	Catalyst mass, segment k, layer n
$A_k$	[m <sup>2</sup> ]	Mass / heat transfer area, channel segment k
$N_C$	[mol/kg]	Specific number of active sites
$\Delta x_n$	[m]	Wall thickness of layer n
$\Delta z_k$	[m]	Length of segment k
$T_g$	[K]	Gas bulk temperature
$T_s$	[K]	Surface temperature
$m_{s,k}$	[kg]	Total mass solid material, channel segment k
$A_s$	[m <sup>2</sup> ]	Catalyst wall cross sectional area
$\Delta H_j$	[J/mol]	Heat of reaction j
$h_k$	[J/s m <sup>2</sup> K]	Heat transfer coefficient, segment K
$q_k$	[J/s m <sup>2</sup> ]	Solid heat flux
$k_c$	[m/s]	Film mass transfer coefficient
$d_P$	[m]	Mean pore diameter
$M_i$	[kg]	Molar mass of specie i
$C_{P,g}$	[J/kg K]	Specific heat capacity, gas
$C_{P,s}$	[J/kg K]	Specific heat capacity, catalyst
$\lambda_g$	[W/m K]	Heat conductivity, gas
$\lambda_s$	[W/m K]	Heat conductivity, catalyst
$d$	[m]	Catalyst channel width
$Sh$	[1]	Sherwood number
$Nu$	[1]	Nusselt number
$T_{ref}$	[K]	Reference temperature
$\Delta t$	[s]	Time step length
$\theta_{ss}$	[1]	Steady state ammonia coverage
$\beta_i$	[1]	Coefficient for implicit method calculations
$\alpha_i$	[1]	Coefficient for first order method calculations
$\tau$	[s]	Characteristic time constant